Contour Detection in High-Resolution Polarimetric SAR Images

Dirk Borghys and Christiaan Perneel and Marc Acheroy

Royal Military Academy, Signal & Image Centre, Renaissancelaan 30, B-1000 Brussels, Belgium

ABSTRACT

Automatic contour detection in SAR images is a difficult problem due to the presence of speckle. Several detectors exploiting the statistics of speckle in uniform regions have been already presented in literature. However, these were mainly applied to multi-look low-resolution imagery. This paper describes two new CFAR contour detectors for high-resolution single-look polarimetric SAR images. They are based on multi-variate statistical hypothesis tests. Failing of the test indicates the presence of an edge. A test for difference in means on log-intensity images and difference in variance on complex (SLC) images are used. Both tests take into account the interchannel covariance matrix which makes them a powerful tool for contour detection in multi-channel SAR images. Spatial correlation jeopardizes the CFAR character of the detectors. This problem is often neglected. In this paper its influence on the detectors is studied and eliminated. The localisation of detected edges is improved using a directional morphological filter. Different methods to fuse the results of the two detectors are explored and compared. Results obtained on a polarimetric L-band E-SAR image are presented. Most contours are well detected. Narrow lines on a uniform background remain undetected. Although the detector was developed to detect edges only between uniform areas, it also detects edges between textured and uniform areas.

Keywords: Edge Detection, Polarimetric SAR, Hypothesis Tests, Multi-variate Statistics

1. INTRODUCTION

The presented work is part of a project that aims at automatically register SAR images with other types of images for remote sensing applications. The general idea is to use a map as an aid for the registration. On a map of the same region as the images the main objects (roads, forests, villages, etc.) are detected automatically. Then, for each type of image, some of the objects found on the map are also detected. Matching the objects provides a first registration. The purpose of the edge detectors presented in this article is thus to automatically find edges between large uniform regions that are likely to be present on maps.

Edge detectors that work well in optical images fail in SAR images. This is due to the particular properties of the speckle in SAR images. The most efficient edge detectors for optical images use a gradient-based method, mostly combined with a smoothening filter. These are well adapted for images with additive noise and a high signal-to-noise ratio (SNR). However, the speckle in SAR has the characteristics of a multiplicative noise (in intensity images) with a very low signal-to-noise ratio. This makes pixel-wise methods using a simple filtering mask inappropriate. Even more elaborate local methods using a combination of an edge detection filter with some smoothening[1,2] give very noisy results.

The solution that is commonly adopted is to take into account larger neighbourhoods of each pixel to decide whether an edge passes through that pixel. This is mostly done using the following principle (Fig. 1): the images are scanned by a set of two adjacent rectangular windows and in each pixel local measurements, which are a function of statistical differences between the pixels in both windows, are used as an indication that the edge between the two windows actually corresponds to an edge in the image. This gives an answer for one possible edge orientation. The set of rectangles is rotated around the current pixel to verify the presence of an edge along other orientations. Mostly 2, 4 or 8 different orientations are tested.

The existing methods were mostly applied on multi-look intensity images and differ by the comparison criterion that is used.

Due to the multiplicative character of the speckle, using the *difference in arithmetic means* as a comparison criterion between the two rectangles yields a detector of which the probability of false alarms increases with the radar reflectivity of the regions.[3] This is a very undesirable property because it means that, in order to obtain a

Further author information: Send correspondence to Dirk.Borghys@elec.rma.ac.be

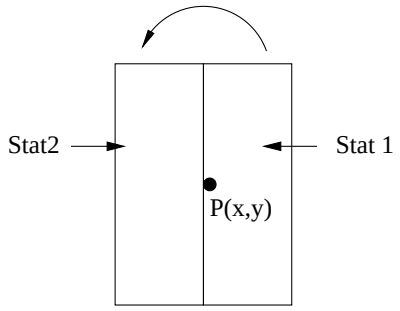

Figure 1. General principle of contour detector

constant false alarm rate (CFAR) detector the threshold used for the detector should be a function of the average intensity around a given pixel. This is very hard to implement. Several solutions are presented in literature. The first is to use the arithmetic average of the log-intensity image. Another possibility is to normalise the difference in means. This can be done by dividing either by the sum of average intensities in both windows or by the empirical standard deviation of both windows These three solutions do provide a CFAR detector.

The most widely used criterion is the *ratio of average intensities*. A detector based on this was proposed by the research teams of Touzi[3] and Bovik.[4] The ratio of average intensities is the maximum likelihood estimation of the ratio of the radar reflectivities in the two rectangles for a single-band SAR image. In that sense the ratio detector is said to be optimal. In[5,6] the ratio detector has been adapted to detect narrow linear features (roads, rivers,...) in SAR images.

Oliver[7,8] proposed a *hypothesis test* as log-likelihood difference to compare the two rectangles in single-look intensity images .

In the current article two new edge detectors for high-resolution polarimetric SAR images are proposed. They are both based on multi-variate hypothesis tests. Contrary to most methods found in literature, we will be working on single-look images instead of multi-look images. Single-look images provide the highest resolution but the maximum strength of the speckle makes the visual interpretation as well as automatic analysis of such images particularly difficult.

Most publications on edge detection in SAR images neglect the problem of spatial correlation and its effect on the developed edge detectors. Correlated speckle in general makes the statistical properties of a detector deviate from the theoretical prediction. When dealing with edge detection in multi-look intensity images, the problem can be circumvented by introducing the notion of equivalent number of looks.[6] Fjörtoft[9,10] solves the problem of spatial correlation by applying a spatial whitening filter as a pre-processing step for edge detection in SLC images.

In the current article the effect of spatial correlation on the two developed detectors is studied. As the developed methods focus on the detection of edges between large uniform regions in high-resolution images it is possible to reduce the effect of spatial correlation by random sub-sampling within the scanning rectangles. For each detector the optimal sampling ratio is determined.

2. TEST IMAGE AND EVALUATION PROCEDURE

The algorithm was tested on an L-Band E-SAR image of the Oberpfaffenhofen area near Munich in Germany. In this article results are presented on a small part of the image, shown in Fig. 2.

In the qualitative evaluation results are shown on the test image. For a more quantitative evaluation the Receiver Operator Curves (ROC) were determined. A ROC is a figure that shows the probability of detection P_d versus the probability of false alarms P_{fa}. The ROC curve is generated by varying the threshold of the detector and each time determining P_d and P_{fa}. The different detectors give relatively wide responses (due to the width of the scanning windows). P_d and P_{fa} were therefore defined as follows:

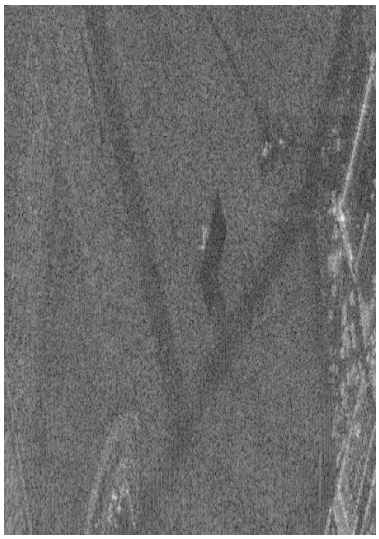

Figure 2. Part of SAR image used as test region for edge detectors

- *Probability of Detection (P_d)*: For a given threshold this is based on the number of pixels in the detector's result image for which the value is above the threshold and the position is within a given distance of the edge. We follow the edges and at each pixel of the edge determine if a detected pixel is close enough. Once such a pixel is found it is set to zero, thus avoiding to count a given pixel twice. The P_d is then defined as the number of detections along the true edge divided by the number of pixels of the edge
- *Probability of False Alarms (P_{fa})*: This is defined as the number of pixels above a given threshold that are not within a given distance ($D > \Delta_{max}$) from a true edge divided by the total number of pixels in the image that are not near an edge.

Please note that the ROC curves depend on the image that is used. It is thus not possible to compare the detectors presented here to other detectors presented in literature on the basis of these ROC curves. When simulated images are used in the evaluation, the contrast-level can be fixed but, as we are dealing with multi-variate data, results will still depend on spatial correlation as well as inter-channel correlation. Comparison of algorithms based on a comparison of results published in articles is therefore very hard.

3. SOME STATISTICAL PROPERTIES OF SAR IMAGES

3.1. Introduction

The primary geophysical quantity determining the appearance of SAR data is the complex radar reflectivity of the imaged surface. This radar reflectivity expresses the fact that, when an electromagnetic wave scatters from a given position of the earth's surface, the physical properties of the terrain cause changes in both the phase and the amplitude of the wave. In distributed targets each resolution cell of the imaging system contains a large number of discrete scatterers. As the wave interacts with the target, each individual scatterer thus contributes a backscattered wave with a phase and amplitude change. The resolution of the SAR system is typically many times the wavelength of the radar, hence, even if all elementary scatterers were identical, they would still produce a very different phase in the incident wave as the waves scattered from them have very different path lengths. As the value of a pixel in the image is determined by the coherent sum of all the scattered waves within a resolution cell, this results in a noise-like characteristic that is called *speckle*. Speckle is found in any image produced by a coherent imaging system (e.g. laser, sonar, ultrasound, radar). The statistical properties of the speckle are very important as they can be used to develop detectors that are well-adapted to SAR images. Another important aspect to be taken into account when developing detection or segmentation methods is correlation: spatial correlation within one image as well as inter-channel correlation. These three topics are briefly discussed in the next paragraphs.

3.2. Distribution of speckle in uniform region of a single-look SAR image

In single-polarisation Single Look Complex (SLC) images the speckle in non-textured uniform regions follows a zero-mean normal distribution and the difference between different uniform regions is characterised by a difference in variance between these distributions.[11] One of the edge detectors presented in this paper is based on this property.

From the complex image other types of images can be determined. Some properties of the statistical distribution of speckle in uniform regions within the different types of commonly used SAR images are presented in table 1. In the log-intensity image the variance in a uniform region is constant, i.e. it is not dependent on the radar reflectivity. Differences in radar reflectivity appear as differences in means. Hence the idea to use a test for difference of means in the log-intensity image for the second edge detector.

Table 1. Speckle distribution in uniform regions of single-look SAR images

Image Type	Definition	Distribution	Remarks
Real, Imaginary	x_r, x_i	Normal	zero-mean
Amplitude	$A = \sqrt{x_r^2 + x_i^2}$	Rayleigh	
Intensity	$I = A^2$	Exponential	$\mu = \sigma$
Log-Intensity	$LI = log(I)$	Fisher-Tippet	$\sigma = c^{st}$

3.3. Spatial correlation

The pixel spacing in SAR systems is always smaller than the resolution cell. This leads to a correlation between neighbouring pixels in the SAR image. Furthermore, as the SAR processing in range and azimuth direction is different, this spatial correlation function is not circular symmetrical as is often the case for optical sensors (visible or infrared). The spatial correlation influences the validity of models used to construct edge detectors. The problem is often neglected. Some authors have incorporated this into the model, leading to very complex methods. This is necessary for low-resolution images. However, when dealing with high-resolution images, the problem can be easily circumvented by sub-sampling the image as long as the number of remaining independent samples is still sufficient for the used segmentation or edge detection method.[11]

3.4. Correlation between the different polarisations

In many articles the correlation between co- and cross-polar polarisations (i.e. HH/HV and VV/HV) is supposed to be zero. This is only the case for objects with azimuthal symmetry. It is thus true in most vegetated areas but not in man-made objects (villages). On the images we received, i.e. L-band images from a region around an airfield, we determined the inter-channel (between the different polarisations) correlation for several types of land-cover as well as for the runway of the airfield. For each type of land-cover the average over a number of examples was taken. Results are presented in table 2.

4. THE PRE-PROCESSING STEP

The distribution of speckle in uniform regions of the polarimetric SLC images follows a zero-mean multi-variate normal distribution. This can be used to locate homogeneous regions in the SAR image, thus limiting the search space for the contour detector. If samples are multi-variate normally distributed, the square of the Mahalanobis distance from the samples to the sample mean follows a χ^2 distribution with degrees of freedom equal to the number of variables.[12] This can be checked using a χ^2-test. We used the test with a 10 % significance level instead of the usual 5 or 1 % levels as we wish to avoid tagging a non-homogeneous region as being homogeneous.

5. THE EDGE DETECTOR BASED ON A DIFFERENCE OF VARIANCE

The contour detector problem is transformed into a multi-variate hypothesis test, the null-hypothesis being that the variance is the same in the two rectangular scanning windows. The statistical test that was used to measure the probability that two sets of variances differ is the Levene test.[12]

Table 2. Correlation coefficients between polarimetric components for various types of land-cover

Type		HH	HV	VV
Village	HH	1.0	0.362	0.809
	HV		1.0	0.389
	VV			1.0
Forest	HH	1.0	0.136	0.186
	HV		1.0	0.136
	VV			1.0
Runway	HH	1.0	0.057	0.389
	HV		1.0	0.129
	VV			1.0
Grass	HH	1.0	0.0449	0.577
	HV		1.0	0.0448
	VV			1.0
Fields	HH	1.0	0.032	0.588
	HV		1.0	0.0144
	VV			1.0

The samples from the two adjacent windows are transformed in absolute deviations of sample means. In the case of a single-look complex polarimetric image with complex data of the type x^{HH}, x^{HV}, x^{VV} this results in:

$$\mathbf{L_{ik}} = \begin{bmatrix} \mid Re(x_{ik}^{HH} - \overline{x}_k^{HH}) \mid \\ \mid Im(x_{ik}^{HH} - \overline{x}_k^{HH}) \mid \\ \mid Re(x_{ik}^{HV} - \overline{x}_k^{HV}) \mid \\ \mid Im(x_{ik}^{HV} - \overline{x}_k^{HV}) \mid \\ \mid Re(x_{ik}^{VV} - \overline{x}_k^{VV}) \mid \\ \mid Im(x_{ik}^{VV} - \overline{x}_k^{VV}) \mid \end{bmatrix}, \tag{1}$$

in which i is the index of the sample and k the index of the rectangular window. The question whether two samples display significantly different amounts of variance is then transformed into a question of whether the transformed values show a significantly different mean.[12] This can then be tested using a Hotellings T^2 test.[13]

The Hotellings T^2 statistic is defined as:

$$T^2 = \frac{n_1 n_2 (\overline{\mathbf{L_1}} - \overline{\mathbf{L_2}})^t \mathbf{C^{-1}} (\overline{\mathbf{L_1}} - \overline{\mathbf{L_2}})}{n_1 + n_2}, \tag{2}$$

where n_1 and n_2 are the number of samples used in both rectangles, $\overline{\mathbf{L_k}}$ is the average $\mathbf{L}$ vector in window k and $\mathbf{C}$ is the pooled covariance matrix defined as:

$$\mathbf{C} = \frac{(\mathbf{n_1} - \mathbf{1})\mathbf{C_1} + (\mathbf{n_2} - \mathbf{1})\mathbf{C_2}}{\mathbf{n_1} + \mathbf{n_2} - \mathbf{2}}. \tag{3}$$

The significance of T^2 is determined by using the fact that in the null-hypothesis of equal population averages the transformed statistic:

$$F = \frac{(n_1 + n_2 - p - 1)T^2}{(n_1 + n_2 - 2)p} \tag{4}$$

follows an F distribution with degrees of freedom p and $(n_1 + n_2 - p - 1)$, where p is the number of variables (i.e. 6 in our case). If we calculate F from the data, we can thus directly associate the probability that the two variances are different to it. However, if the F-statistic (4) is calculated using all pixels in the rectangular windows,

the experimentally found 5 % threshold, for a uniform region, is higher than the theoretically predicted one. This was shown to be due to the spatial correlation of the samples within the scanning windows.[14] In order to check this, we constructed a set of 15 simulated images with a zero-mean multi-variate normal distribution, without spatial correlation but with inter-channel correlations and variances that are comparable to those actually found in some uniform regions in the SAR image.

For these test images we have calculated the 5 % threshold as a function of sampling ratio for sampling with and without replacement. The results are shown in Fig. 3(left). When less than 10 % of the points are considered, both sampling schemes are nearly equivalent and their values correspond to the theoretical threshold. However, as the number of selected points increases, the threshold for sampling with replacement increases while the one for sampling without replacement slightly decreases. In fact the behaviour for the sampling without replacement corresponds to the theoretical behaviour of the threshold as shown in Fig. 3. The figure shows the average thresholds $\overline{T}$ over the 15 windows for both sampling schemes as well as $\overline{T} \pm \sigma_T$ (dotted lines). The fact that in the case of sampling with replacement the threshold increases can be explained by the fact that the replacement itself introduces a correlation between the samples.

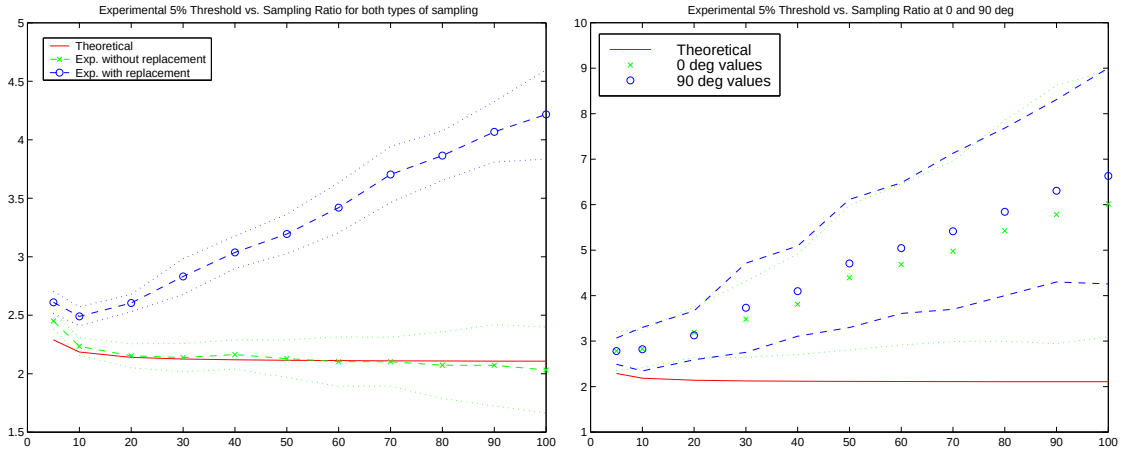

Figure 3. 5% Threshold vs. sampling ratio for sampling with and without replacement in simulated images without spatial correlation (left) and for sampling without replacement in uniform regions of the SLC SAR image (right)

We have thus established that sub-sampling without replacement reduces the effect of correlation. Now we would like to determine what is the maximum sampling ratio allowed to have results that are useful. Two things need to be checked:

- Do the data indeed follow an F-distribution ?
- Is it possible to assign a constant false alarm threshold independent of the average radar reflectivity of the uniform region?

The answer to these two questions was found by studying the behaviour of the F-statistic defined by equation 4 in 15 uniform regions of the SAR image corresponding to different radar reflectivities. For each region an F-distribution was fitted through the data. A χ^2-test was used to compare the "experimental" F-distribution with the theoretical one. For sampling ratios below 20 % the two distributions are equal (with a significance level of 5 %). At 30 % sampling rate the distributions are only equal if the rectangles are horizontal (as the largest spatial correlation was found to be in the vertical direction, the degradation of the model appears faster using vertical windows). So, sampling should be lower than 30 %.

To answer the second question, the 5 % threshold level was determined experimentally from the histograms of the F-statistic in the 15 uniform regions as a function of sampling rate. The average and standard deviation over the 15 regions was determined. Results are shown in Fig. 3(right) for both horizontal and vertical windows. From the figure

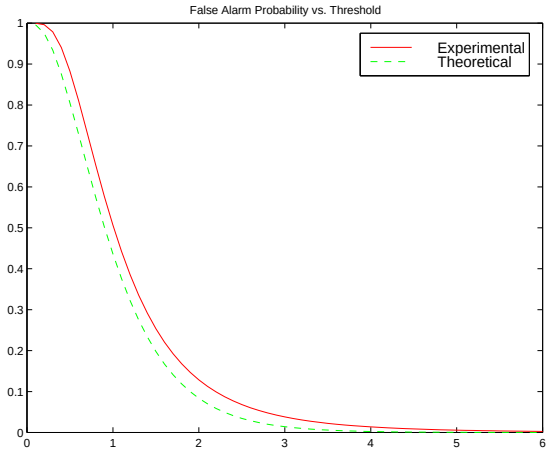

Figure 4. False alarm probability vs. threshold for experimental and theoretical F-distribution

it appears that it is only possible to assign a global threshold corresponding to a given probability of false alarms for all directions when 10 % or less of the points within the window are used to calculate the statistic. Otherwise a threshold has to be set for each direction separately and the method is not valid above 20 % sampling. The detector will thus sample at 10 % and the threshold will be derived from the average experimental F-distribution (see Fig. 4). As we are only interested in finding contours of large regions, large scanning rectangles can be used. We used 51×11 rectangular windows. For such windows, a 10 % sampling rate still provides enough independent samples for the method to be valid.

6. THE EDGE DETECTOR BASED ON A DIFFERENCE IN MEANS

The idea is to apply a multi-variate test for difference in means between two populations. The hottellings T^2 test[12] that was mentioned before was used. The log-intensity image is the best candidate for comparing regions on the basis of this test because differences in radar reflectivity are reflected in these image purely as variations of means and because the form of the distribution is independent of the radar reflectivity. In order to check the validity of this detector similar tests were performed as for the first detector.

In simulated images without spatial correlation the threshold again corresponds to the theoretically predicted one.

In Fig. 5 (left) the 5 % threshold is plotted versus the sampling ratio for the 15 uniform regions, this time in the Log-Intensity SAR image. The theoretical threshold is lower than the one that was found experimentally for all sampling ratios. The relative variation of the threshold over the different test windows decreases as the sampling ratio decreases. This is illustrated by Fig. 5(right) where the ratio between the standard deviation and the average of the experimental 5 % false alarm threshold is plotted as a function of the sampling ratio. At a sampling ratio of 10 % this ratio is smallest. At 5 % sampling the ratio increases again because the number of samples is getting too small (< 30). We will thus apply the detector with a sampling ratio of 10 %. However, the probability of false alarms is always higher than the theoretically predicted one. The CFAR thresholds are determined experimentally from simulated Fisher-Tippet distributed data with the same spatial correlation as the SAR image.

7. IMPROVEMENT OF EDGE LOCALISATION

Edge detectors based on differences between two adjacent scanning windows result in blurred edges. In order to sharpen these edges we used a directional morphological operator. As the detectors provide a response for each orientation of the set of scanning rectangles the approximate orientation of candidate edges is known a priori and this information is used in the filter. We have adapted the morphological filter presented by Chanussot.[15] The first step fills small gaps in the contour detector's result image. This can be done by a closing with reconstruction[15] but we have obtained better results using a median filter. In each pixel the median is calculated inside an elongated

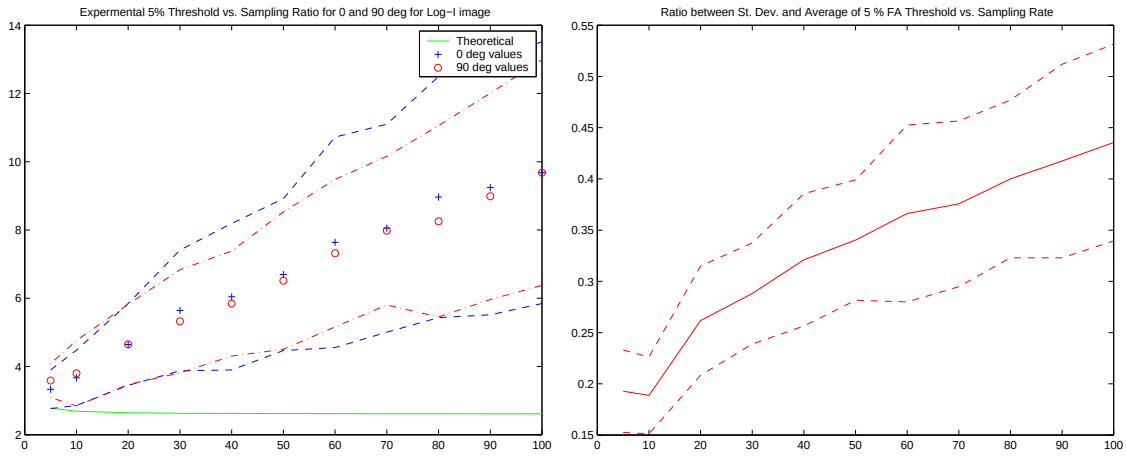

Figure 5. 5% Threshold vs. sampling ratio for sampling without replacement in uniform regions of the Log-Intensity SAR image (left) and Ratio of standard deviation to average of the 5 % threshold vs. sampling ratio

rectangular array around that pixel. The maximum response is obtained if the rectangle is oriented in the direction of the edge. The maximum is determined over a small range of orientations around the orientation of the detector's masks. This step thus combines smoothening with the filling of small gaps. The next two steps do follow the approach presented by Chanussot[15]: The supremum of directional openings is used to remove nonlinear or too short mountains in the detector response. A closing with a small (5×5) structuring element is used to remove some other isolated false alarms. The last step is an erosion to further narrow the result. In Fig. 6 the results of the some steps of this morphological filter are shown on a small (32×32) part of the test image.

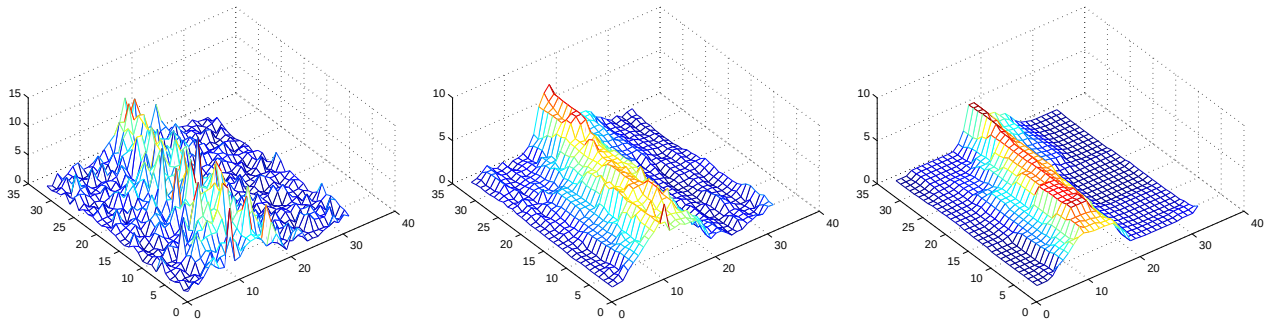

Figure 6. Results of morphological filter: Left: Original response of (Levene) detector, Centre: Result of directional median filter, Right: Final result

8. COMBINATION OF THE RESULTS OF THE EDGE DETECTORS

8.1. Combining the results for different directions of the processing window

Up-to now we have been working with the responses of the edge detectors for each orientation of the scanning window separately. In order to obtain a final edge map the results for the different orientations need to be combined. Several ways to do this are suggested in literature[10]:

- Sum: Summing the results from all orientations which is equivalent to the taking average
- Maximum: Keep the maximum over all orientations

- Generalised Norm: Expand the notion of norm to multiple orientations[10]: $E_f = \sqrt{\sum_{i=1}^{N/2} \frac{E^2(\alpha_i)+E^2(\alpha_i+90^\circ)}{2}}$ with N the number of orientations and $E(\alpha_i)$ the detector's response at orientation α_i.

A ROC curve was constructed for these 3 combination methods for the Levene and the Hotellings test. The ROC curves were calculated based on the results obtained in the real test image (Fig. 2). For the performance measured by these ROC curves the sum and the generalised norm give exactly the same results. The maximum gives a lower probability of detection at low false alarm rates. We will thus use the sum of the directional responses.

8.2. Combining the results of the two detectors

The fusion of different edge detectors can be done at several levels:

- Vectorise the results and fuse the resulting vectorised objects
- Fuse the thresholded image of each detector after combining the results for different directions
- Fuse the results for each direction separately

If the edges are vectorised before fusion the fusion is limited to some voting mechanism. Furthermore, the vectorisation imposes some constraints on the edges and this can result in a lower detection rate. The second and third possibilty are almost equivalent but the last fusion strategy automatically ensures that only edges that were found by both detectors to have a similar orientation, are fused. This is the method that we used.

In order to fuse the results of the two detectors, these results should be rescaled such that they represent comparable values, i.e. it makes no sense combining the values of the output directly as they correspond to different significance levels for detection. The relation between the detector's threshold and the probability for false alarms (e.g. Fig. 4for the Levene Test) can be used to rescale each detector's output.

For the moment two fusion methods were tested. The first method is based on geodesic reconstruction.[15] The idea is that the ideal result of fusion lies between the maximum and the minimum of the different detectors. If all detectors detect an edge at a given position, the minimum and maximum are both high and close together. This gives a high confidence in the presence of an edge in that point. If such a point is found in the image it is likely that some neighbouring points also belong to an edge. Even if only one detector would confirm this. The proposed fusion thus starts from the minima as markers that are dilated until they coincide with the maximum, i.e. starting from the minima of all detector's responses a dilation is iteratively executed until idempotence with the maximum.

Generally the false alarm thresholds used for the individual edge detectors vary from 1 to 5 %. Three input membership functions were defined accordingly (see Fig. 7). Five output classes, corresponding to an increasing edge strength, were defined. Some of the rules used to combine the results of the two detectors are given in table 3. The minimum is used both as the combination and the implication operator. Centroid defuzzification was used to get the final score.

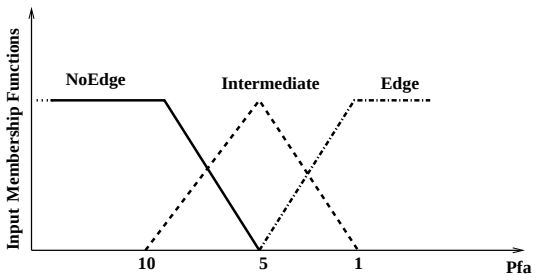

Figure 7. Input Membership Functions

Table 3. Rules for combining the results of the two multi-variate edge detectors

if	(Levene=NoEdge)	and	(Hotelling=NoEdge)	then	(Output=NoEdge)
if	(Levene=NoEdge)	and	(Hotelling=Intermediate)	then	(Output=WeakEdge)
if	(Levene=Intermediate)	and	(Hotelling=Intermediate)	then	(Output=MediumEdge)
if	(Levene=NoEdge)	and	(Hotelling=Edge)	then	(Output=MediumEdge)
if	(Levene=Intermediate)	and	(Hotelling=Edge)	then	(Output=Edge)
if	(Levene=Edge)	and	(Hotelling=Edge)	then	(Output=StrongEdge)

9. RESULTS AND DISCUSSION

In order to compare the two edge detectors a set of test images with a vertical edge was simulated (having the correct spatial correlation and speckle distributions) and the ROC curve was determined for both detectors with the scanning rectangles in the direction of the edge. The simulated images have varying contrast over the edge. The resulting ROC curves are shown in Fig. 8(left). From the ROC curves it can be concluded that none of the two detectors is best over the complete range, i.e. the curve for the Levene test crosses the one for the Hotellings test and the point where this crossing occurs depends on the contrast. This means that, even if the false alarm rate is fixed, it is not possible to say that one detector is better than the other one, because this will depend on the contrast of the edges in the image. It is thus not possible to decide a priori which test is better and it is necessary to fuse the results of both detectors.

Based on the two fusion operators discussed in the previous section four different fusion methods were tried. The first three use geodesic reconstruction as the fusion operator. In the first method there is no morphological thinning. In the second the morphological filter is applied after the fusion and in the third before. The fourth method uses the fuzzy inference system after morphological filtering. In Fig. 8(right) the ROC curve for the 4 methods is shown. As a reference the result of the two individual detectors is also shown. If the morphological filter is not used, results after fusion are worse than for the individual detectors. The fusion based on fuzzy inference provides slightly better results than the other method.

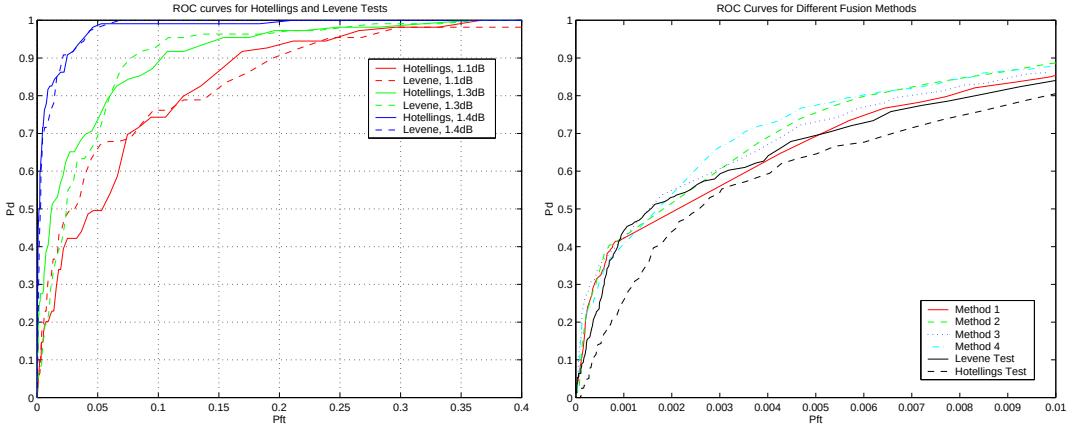

Figure 8. ROC curves for individual detectors at vaying contrast levels in simulated images (left) and comparison of the 4 fusion methods applied on a real test image (right)

In order to obtain vectorised results a bar detector[2] was applied on the thresholded responses of the detectors or after the fusion. In Fig. 9 the vectorised results for the two individual detectors at the 5 % false alarm threshold are shown as well as the result of the fusion by fuzzy inference (after a 50 % threshold). Some false alarms persist. These could be filtered out using higher-level tools that ensure the continuity of edges. The detectors give good results for detecting edges between large regions. However, crossings of edges are sometimes missed and if the concentration of

edges is high, as in the built-up area on the left of the image, the detector performs poorly. The localisation of edges should thus be improved.

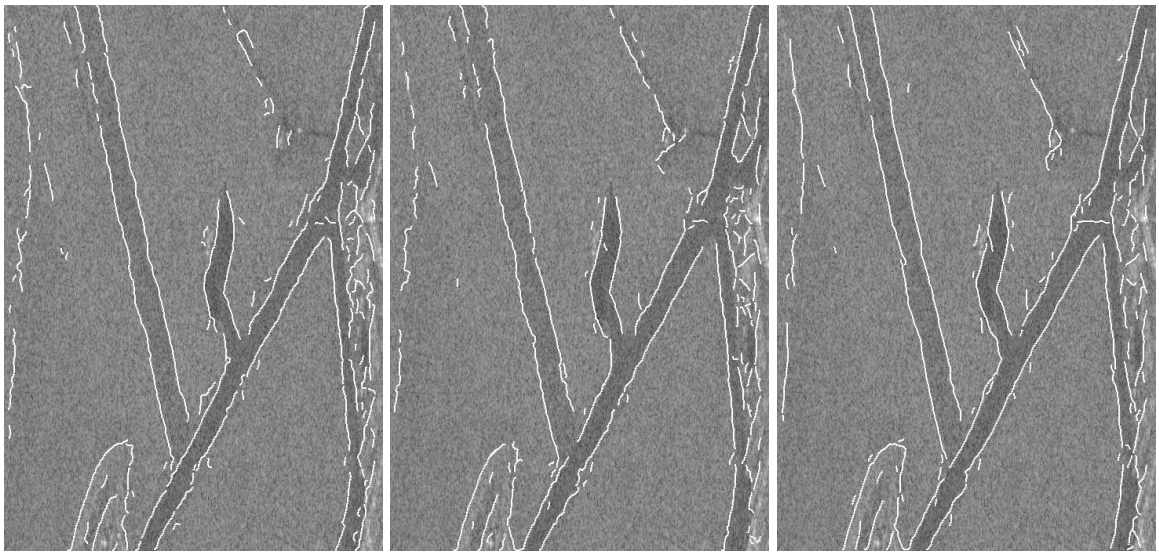

Figure 9. Vectorised results for Levene test (left), Hotellings test (centre) and Fuzzy Fusion (right)

ACKNOWLEDGMENTS

The presented work is the result of a collaboration between the Signal & Image Centre of the Belgian Royal Military Academy and the Institut für Hochfrequenztechnik und Radarsysteme of the Deutshes Zentrum für Luft- and Raumfahrt (DLR), who also provided the images. The images used in this project are acquired by DLR's E-SAR system.

10. CONCLUSIONS

In this article two new edge detectors for single-look high-resolution polarimetric SAR images are presented. The presented work is part of a project aiming to automatically register SAR images with maps and other images. The first step is the registration between the SAR image and a map. The edge detectors are therefore designed to detect edges between large areas that are likely to be also present on maps.

Both developed detectors are based on a multi-variate hypothesis test. The first one tests a difference in variance and is applied to the complex image. The second one tests a difference in means and is applied to the log-intensity image. The detectors seem to be complementary. Different methods to fuse their results are presented and compared. Of the proposed methods, the fusion based on a fuzzy inference system gives the best results. Other fusion methods should be tried though.

Both detectors give good results for detecting edges between large areas. However, crossings of edges are sometimes missed. Furthermore, in areas where the concentration of edges is very high (e.g. built-up areas) the detectors only find a small portion of the edges that are present. Although the detector is not designed for this case, it could perhaps cope with such regions. In general the localisation of edges should be improved. The best algorithm to do that depends on the type of area in the image. For completing edges of fields a method based on active contours[16] could be used. For finding the location of edges in built-up areas either another type of detector (e.g.[5]) should be used or the edge map should be improved using for example watersheds.[10] The information about the type of area will be provided by the map.

One of the ideas that will be pursued further is to first use the edges between large areas together with other information, such as the location of built-up areas[17] or forests to find a first registration between the image and the

map and then use the information from the map to improve the results of the edge detection on the SAR image. This will allow to refine the registration with the map and to obtain a registration between different images (using e.g. the edges of different agricultural areas).

REFERENCES

1. J. Canny, "A computational approach to edge detection," *IEEE-PAMI* **8**, pp. 679–697, 1986.
2. V. Lacroix and M. Acheroy, "Feature extraction using the constrained gradient," *ISPRS Journal of Photogrammetry & Remote Sensing* **53**, pp. 85–94, April 1998.
3. R. Touzi, A. Lopes, and P. Bousquet, "A statistical and geometrical edge detector for sar images," *IEEE-GRS* **26**, pp. 764–773, November 1988.
4. A. Bovik, "On detecting edges in speckle imagery," *IEEE-ASSP* **36**, pp. 1618–1626, October 1988.
5. F. Tupin, H. Maitre, J. Mangin, J. Nicolas, and E. Pechersky, "Detection of linear features in sar images: Application to road network extraction," *IEEE-GRS* **36**, pp. 434–453, March 1998.
6. F. Tupin, *Reconnaissance des Formes et Analyse de Scènes en Imagerie Radar à Ouverture Synthétique*. PhD thesis, ENST, Paris, September 1997.
7. C. Oliver, "Edge detection in sar images," in *Proc. of the 1994 Data Processing for Remote Sensing*, vol. 2316, pp. 80–91, SPIE, SPIE, April 1994.
8. C. Oliver, D. Blacknell, and R. White, "Optimum edge detection in sar," *IEE Proc Radar, Sonar, Navig.* **143**, pp. 31–40, February 1996.
9. R. Fjörtoft, A. Lopes, J. Bruniquel, and P. Marthon, "Optimal edge detection and edge localization in complex sar images with correlated speckle," *IEEE-GRS* **37**, September 1999.
10. R. Fjörtoft, *Segmentation d'images radar par detection de contour*. PhD thesis, Institut National Polytechnique de Toulouse, Toulouse, March 1999.
11. C. Oliver and S. Quegan, *Understanding Synthetic Aperture Radar Images*, Artech House, Boston-London, 1998.
12. B. Manly, ed., *Multivariate Statistical Methods*, Chapman and Hall, 1995.
13. T. Anderson, *Introduction to Multivariate Statistical Analysis*, John Wiley & Sons, New York, 1958.
14. D. Borghys, C. Perneel, and M. Acheroy, "A multi-variate contour detector for high-resolution polarimetric sar images," in *International conference on Pattern Recognition, Barcelona*, sept 2000.
15. J. Chanussot, G. Mauris, and P. Lambert, "Fuzzy fusion techniques for linear features detection in multitemporal sar images," *IEEE-GRS* **37**, pp. 1292–1305, May 1999.
16. O. Germain and P. Réfrégier, "Edge detection and localisation in sar images: a comparative study of global filtering and active contour approaches," in *Europto Symp. on Remote Sensing*, vol. 3502, pp. 111–121, SPIE, SPIE, (Barcelona, Spain), September 1998.
17. D. Borghys, C. Perneel, and M. Acheroy, "Detection of built-up areas in polarimetric sar images," in *First International Workshop on Pattern Recognition in Remote Sensing; Andorra*, sept 2000.